NASA TN D-1535

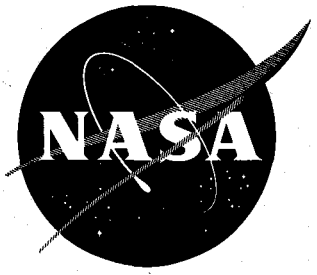

TECHNICAL NOTE

D-1535

HEAT TRANSFER TO A SPHERE WITH A RETROROCKET EXHAUSTING INTO A FREE STREAM; MACH 2.0 AND 0.8

By Robert A. Wasko

Lewis Research Center
Cleveland, Ohio

NATIONAL AERONAUTICS AND SPACE ADMINISTRATION
WASHINGTON
November 1962

NATIONAL AERONAUTICS AND SPACE ADMINISTRATION

TECHNICAL NOTE D-1535

HEAT TRANSFER TO A SPHERE WITH A RETROROCKET EXHAUSTING INTO A FREE STREAM; MACH 2.0 AND 0.8

By Robert A. Wasko

SUMMARY

A 9.3-inch-diameter sphere with a flush mounted lox - JP-4 retrorocket was tested in the Lewis 8- by 6-foot tunnel at free-stream Mach numbers of 2.0 and 0.8, angles of attack of 0°, -5°, -10°, and -20°, chamber pressures of 150, 200, and 300 pounds per square inch absolute, and oxidant-fuel ratios of 2.1 to 2.5.

The results indicated more severe heating at Mach 2.0 than at 0.8 with only a slight effect on heat transfer because of variation in oxidant-fuel ratio. Heating rates decreased downstream from the nozzle exit at both Mach numbers. Increasing the angle of attack at Mach 2.0 decreased the heat flux on the windward (top) surface and side of the sphere but increased it on the leeward (bottom) surface. At Mach 0.8, increasing the angle of attack decreased the heat flux on all portions of the sphere although the leeward-surface values were highest. Increases in chamber pressure for an angle of attack of -5° increased the heat flux on all portions of the model surfaces at Mach 2.0, whereas at Mach 0.8 a similar but smaller effect occurred. Chamber pressure increases at Mach 0.8 and zero angle of attack generally decreased the heat flux. Jet-on surface pressures were less than jet-off values at both Mach numbers, but reductions at Mach 2.0 were greater than at 0.8. Increasing chamber pressure had no effect on the pressure distribution at Mach 0.8.

INTRODUCTION

The use of retrorockets has been considered as a decelerating technique for the control of flight velocity and attitude of space vehicles that have entered an atmosphere. Reference 1 discusses the modulation of aerodynamic properties by a centrally located retrojet. The present study investigated heating resulting from the interaction of the retrorocket gases and the free stream.

A 9.3-inch sphere with a flush mounted lox - JP-4 rocket motor was investigated in the Lewis 8- by 6-foot tunnel at free-stream Mach numbers of 2.0 and

0.8 for a range of angle of attack from 0° to -20°. Distributions of heat flux, heat-transfer coefficients, and recovery temperatures as well as static pressures were obtained around the model circumference for variations in combustion-chamber pressures and oxidant-fuel ratios.

SYMBOLS

h heat-transfer coefficient

M_0 free-stream Mach number

P_c combustion-chamber pressure

p_l local static pressure

p_0 free-stream static pressure

$\dot{Q}$ heat flux

T absolute temperature

T_r recovery temperature

α angle of attack

APPARATUS

Figure 1(a) is a schematic diagram of the model in the tunnel. The stationary transonic strut supported the sting-mounted model, and lox and JP-4 fuel lines as well as instrumentation leads were brought down to the model through the propellant strut. The angle of attack was achieved by pivoting the model centerline about a center of rotation located just downstream of the sphere. The rocket engine (fig. 1(b)) was a modification of that described in reference 2 and had a conical nozzle with an area ratio of 4. The average value of characteristic velocity c^* was 4500 feet per second.

The calorimeters and the static-pressure orifices were located symmetrically on the top, bottom, and side of the sphere as indicated in figure 2(a). As shown in figure 2(b), two Chromel-Alumel thermocouples, silver soldered to the disk, supported the copper calorimeters to minimize conduction losses; two thermocouples were used in the event that one failed. Nitrogen purge air was used to cool the calorimeters and to eliminate deposition of contaminants during the motor starting sequence. The copper disks were blackened in an effort to obtain total heat flux, and no attempt was made to determine the convective and radiative components independently.

PROCEDURE

Motor Operation

Ignition of the rocket motor was accomplished in the following way: Triethyl aluminum (a pyrophoric) was injected into the combustion chamber with gaseous oxygen for approximately 2 seconds. Then, partial propellant flows were injected for 6 seconds and ignited by the pilot flame. The propellant flows were gradually increased to full flow, and after approximately 4 seconds full chamber pressure was obtained.

Data Acquisition

From heat transfer theory, it follows that the steady-state heat transfer to the disk by the hot gas is given by

$$\dot{Q} = h(T_{gas} - T_{disk})$$

The disk absorbs heat according to

$$\dot{Q} = \rho C t \frac{dT_{disk}}{d\theta}$$

where ρ is density, C is specific heat, t is thickness, and θ is time.

Since the copper disk is thin and has a high conductivity, the thermocouple temperature is essentially equal to the disk temperature. If reradiation from the disk is assumed to be small, the disk heat flux is equal to the heat flux from the gas and

$$\rho C t \frac{dT_{disk}}{d\theta} = h(T_{gas} - T_{disk})$$

An analog differentiating circuit and X-Y plotter were employed to chart calorimeter heating rates against disk temperature. Figure 3 shows sample traces for two calorimeters. From the previous discussion it is clear that for the linear portion of the trace the heat-transfer coefficient would be the slope of the curve when the gas temperature is assumed constant; that is,

$$\frac{\dot{Q}_2 - \dot{Q}_1}{(T_{gas} - T_{disk})_2 - (T_{gas} - T_{disk})_1} = \frac{\dot{\Delta Q}}{\Delta T_{disk}}$$

The recovery temperature is defined as that temperature at which the heat flux is zero. It was obtained by extrapolating the trace to intersect the abscissa. For convenience the heat-flux data presented in later figures correspond to an arbitrary disk temperature of 100° F, which was obtained by extending the trace toward the ordinate. The heat-flux trends observed are assumed valid for other disk temperatures.

It must be realized that, in general, the spherical surface and the calorimeter disk are at different temperatures and a nonisothermal wall situation exists (see ref. 3). Hence the absolute magnitude of the heating results (particularly the recovery temperature) will be influenced somewhat by the spherical-surface heat-sink effects. Therefore the absolute magnitude of the results is of nebulous value, but the order of magnitude as well as the trends in the data are useful observations.

RESULTS

Heat Transfer

The effect of Mach number on circumferential distribution of surface heat transfer at zero angle of attack is shown in figure 4 for a chamber pressure of 200 pounds per square inch absolute. At Mach 2.0 the heat flux was maximum near the nozzle exit and decreased rapidly farther downstream. The heat flux was substantially less at Mach 0.8 but again was greatest near the nozzle exit. The slight asymmetry in heat flux values on the top, bottom, and side of the sphere at Mach 2.0 may have been a result of slight model misalinement with the tunnel flow. The heat-transfer coefficients were not symmetrical at either Mach number, and no consistent trend was evident. The variations in recovery temperatures were similar to those of the heat flux at both Mach numbers and the distributions were symmetrical.

Variation in oxidant-fuel ratio produced very little effect at Mach 0.8, as shown in figure 5. A slight tendency toward decreasing heat flux and recovery temperature occurred with increases in oxidant-fuel ratio.

The effect of angle of attack is shown for Mach 2.0 and 0.8 in figures 6(a) and (b), respectively. At Mach 2.0, increasing angle of attack from zero to -5° decreased the heat flux and recovery temperatures on the top (windward surface) and side of the sphere and increased them on the bottom (leeward surface). The side data appeared to be highest at zero but intervened at the top and bottom data at -5°. At an angle of attack of -20°, further increases in heat flux on the bottom occurred only near the nozzle exit, while values toward the rear were less than the zero-angle-of-attack data and top and side values were nearly zero. Generally, the heat flux and recovery temperature decreased downstream from the nozzle exit. The results at Mach 0.8 show that as the angle of attack increased from zero to -5° the heat flux decreased on the top and side of the sphere but changed little on the bottom. At -10° heating occurred only on the bottom of the sphere; therefore, heat-transfer coefficients and recovery temperatures were not obtained on the top and the side. At all angles of attack the magnitudes of heat flux and of recovery temperature were nearly constant around the sphere.

The effect of variation in chamber pressure at Mach 2.0 and 0.8 is shown in figure 7. At Mach 0.8 and zero angle of attack (fig. 7(a)), increasing the chamber pressure generally resulted in decreases in heat flux and recovery temperature. At an angle of attack of -5° (fig. 7(b)), increasing chamber pressure resulted in decreasing heat flux and recovery temperature on the bottom

surface, while the top and side values tended to increase. Figure 7(c) shows that at Mach 2.0 and an angle of attack of -5°, increasing the chamber pressure resulted in increasing heat flux and recovery temperature on the top, side, and bottom of the sphere. Maximum values of heat flux, heat-transfer coefficient, and recovery temperature recorded during the test are indicated in the figure as 44 Btu per square foot per second, 0.08 Btu per square foot per second per °F, and 1060° F, respectively, at Mach 0.8; and 250 Btu per square foot per second, 0.1 Btu per square foot per second per °F, and 2950° F, respectively, at Mach 2.0.

Photographs of test firings at both Mach numbers are shown in figure 8 for angles of attack of zero and -5°. The change in jet shape with Mach number is apparent and indicates the difference in heating between Mach 2.0 and 0.8. Deflection of the jet toward the leeward side of the sphere during operation at angle of attack is particularly evident at Mach 2.0.

Pressures

The effects of Mach number and angle of attack on circumferential pressure distributions are shown in figure 9. At Mach 2.0 (fig. 9(a)) jet-off pressure distributions show an increase on the windward surface and a decrease on the leeward surface for increases in angle of attack except towards the rear of the sphere (~120°) from nozzle exit). Side pressures changed very little. The reduction in jet-on pressures at zero and at -5° angle of attack is a result of the jet acting as an aerodynamic spike and reducing bow wave pressures to oblique shock pressures. (See ref. 1 for a description of this phenomenon.) At an angle of attack of -20° top-surface pressures approached jet-off values.

At Mach 0.8 (fig. 9(b)), jet-off pressure variations with angle of attack were similar to those at Mach 2.0 but of smaller magnitude. Jet-on pressure distributions were fairly constant for angles of attack of zero and -5° and were nearly reduced to jet-off downstream surface pressures. At -10°, however, the top pressures were the same as the jet-off values, whereas the bottom pressures were less than jet-off values. No significant change was evident with a variation in chamber pressure.

SUMMARY OF RESULTS

A 9.3-inch-diameter sphere with a flush mounted lox - JP-4 retrorocket was tested at free-stream Mach numbers of 2.0 and 0.8 for angles of attack of 0°, -5°, -10°, and -20° at chamber pressures of 150, 200, and 300 pounds per square inch and oxidant-fuel ratios of 2.1 to 2.5. Spherical surface heat-transfer and pressure data indicated the following results:

1. The total heat transfer was more severe at Mach 2.0 than at 0.8. At Mach 2.0, the maximum value of heat flux (for a disk temperature of 100° F) was 250 Btu per square foot per second, the maximum heat-transfer coefficient was 0.1 Btu per square foot per second per °F, and the maximum recovery temperature

was 2950° F. Values at Mach 0.8 were 44 Btu per square foot per second, 0.08 Btu per square foot per second per °F, and 1060° F. Heating rates decreased downstream from the nozzle exit at both Mach numbers.

2. At Mach 0.8 variation in oxidant-fuel ratio had only a slight effect on heat transfer.

3. For increasing angles of attack, the heat flux at Mach 2.0 decreased on the windward surface and side of the sphere and increased on the leeward surface. At an angle of attack of -20°, the heat flux increased only on the leeward surface near the nozzle exit. Increasing angle of attack at Mach 0.8 decreased the heat flux on all portions of the sphere, although the leeward surface values were highest. At -10° heating occurred only on the leeward surface.

4. Increasing chamber pressure at Mach 0.8 for zero angle of attack generally tended to decrease the heat flux on all surfaces. At an angle of attack of 5°, values on the leeward surface decreased, whereas the windward surface and side heating rates tended to increase. Increasing chamber pressure at Mach 2.0 for a 5° angle of attack resulted in increased heat flux on all portions of the model surface.

5. Jet-on sphere-surface pressure distributions at Mach 2.0 were reduced considerably from jet-off values, particularly for angles of attack near 5°. Reductions in jet-on surface pressures at Mach 0.8 were not as large as the Mach 2.0 reductions. At Mach 0.8 increasing chamber pressure did not affect the pressure distributions.

Lewis Research Center
National Aeronautics and Space Administration
Cleveland, Ohio, September 10, 1962

REFERENCES

1. Charczenko, Nickolai, and Hennessey, Katherine W.: Investigation of a Retrorocket Exhausting from the Nose of a Blunt Body into a Supersonic Free Stream. NASA TN D-751, 1961.

2. Stein, Samuel: A High-Performance 250-Pound-Thrust Rocket Engine Utilizing Coaxial-Flow Injection of JP-4 Fuel and Liquid Oxygen. NASA TN D-126, 1959.

3. Rubesin, Morris W.: The Effect of an Arbitrary Surface-Temperature Variation Along a Flat Plate on the Convective Heat Transfer in an Incompressible Turbulent Boundary Layer. NASA TN 2345, 1951.

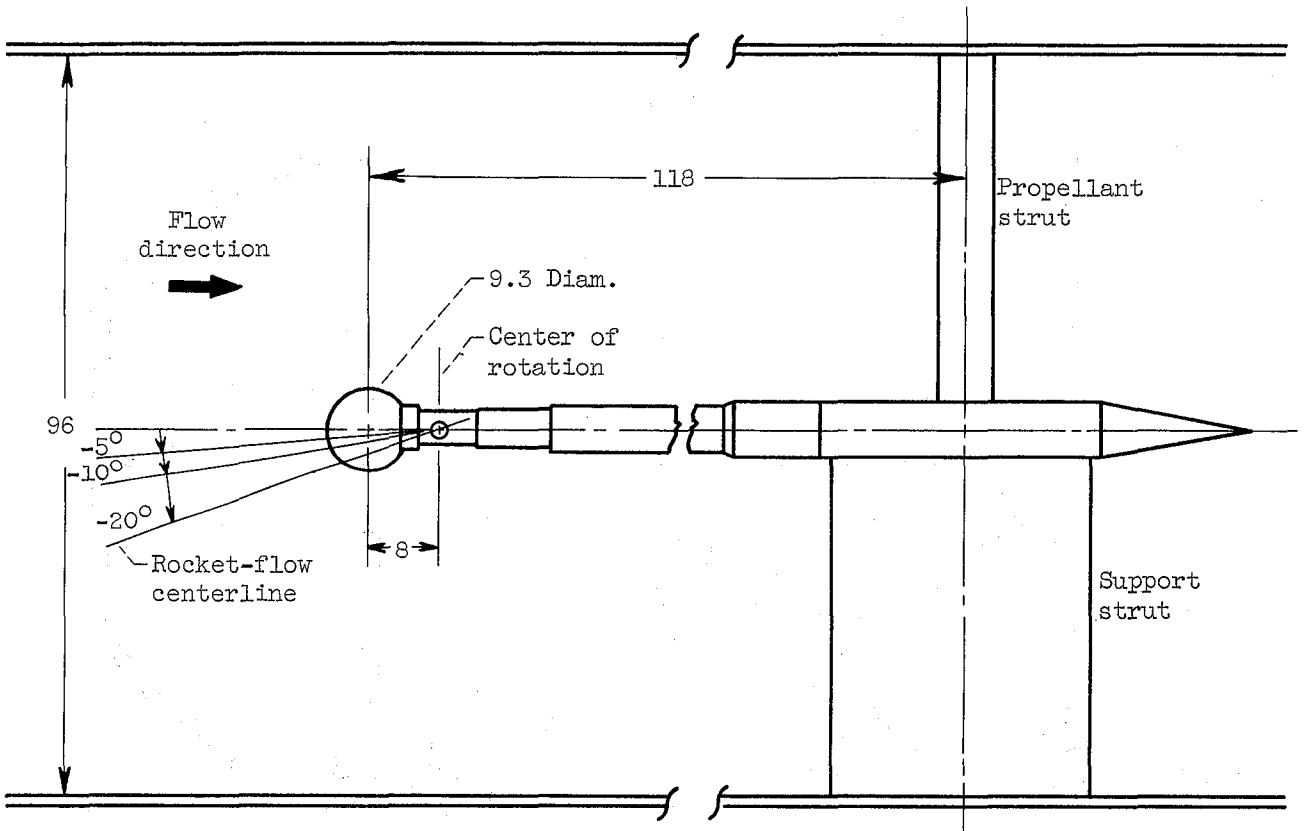

(a) Schematic diagram of model in tunnel.

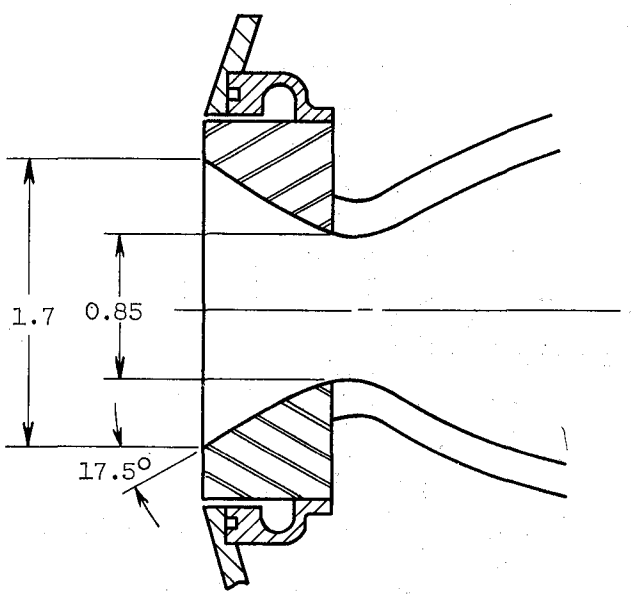

(b) Rocket engine.

Figure 1. - Details of model. (Dimensions in inches.)

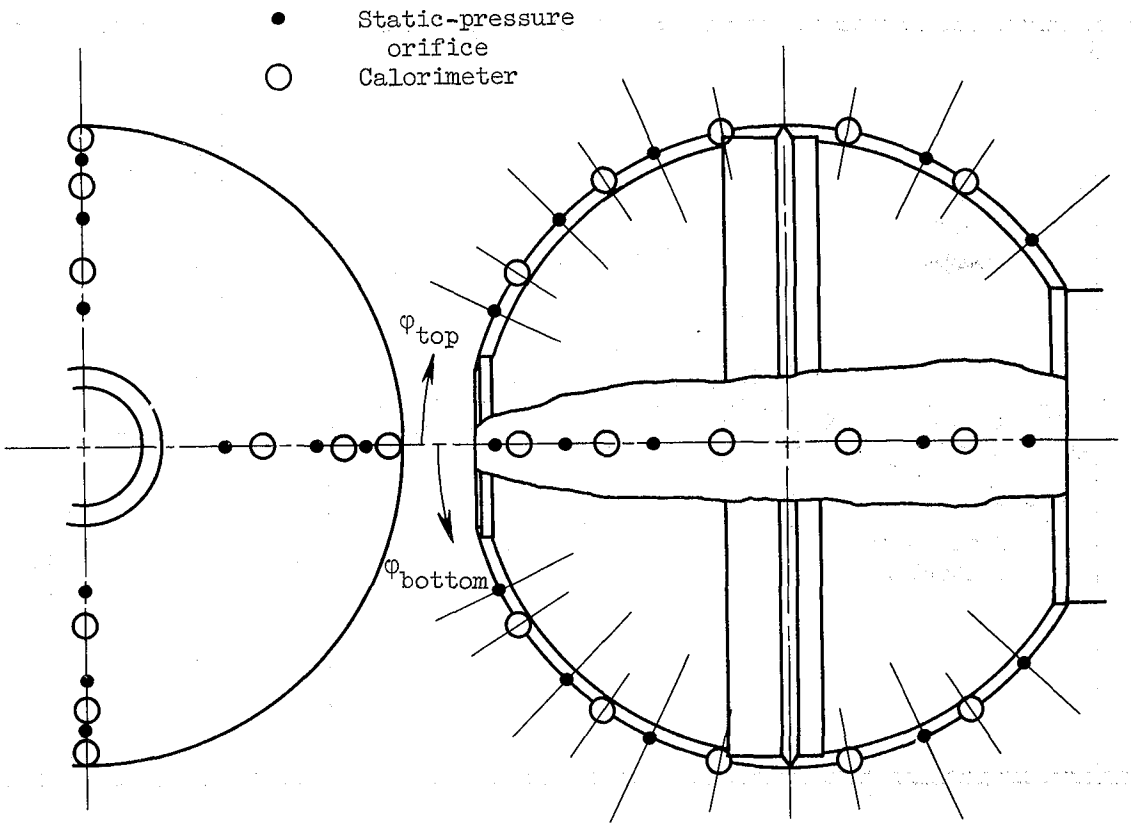

(a) Location of calorimeters and static-pressure orifices.

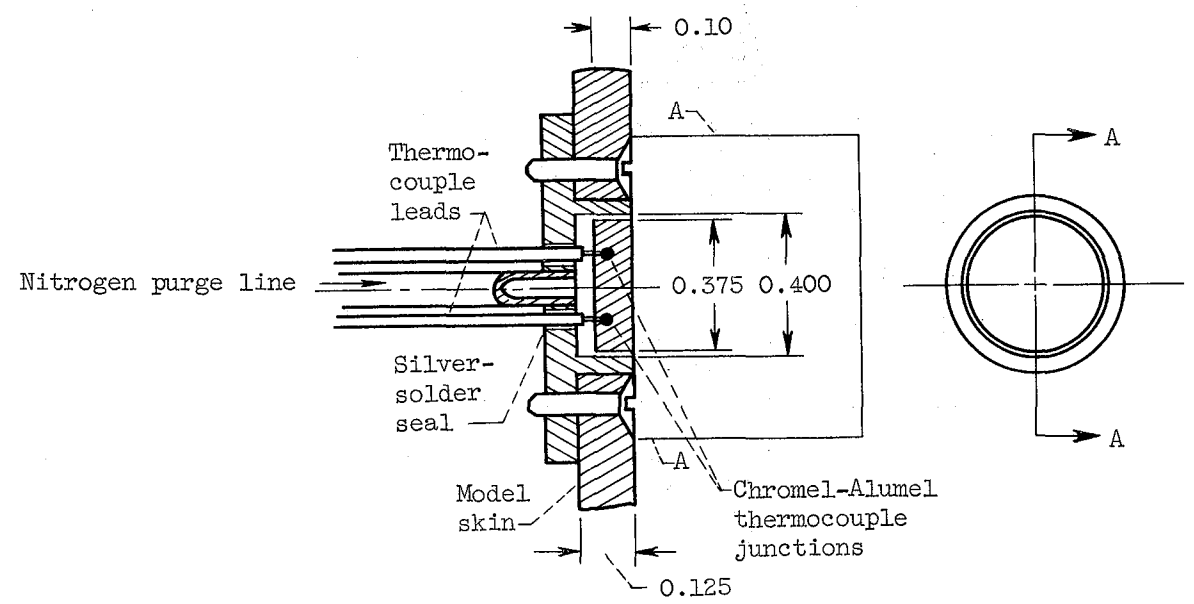

(b) Copper-disk calorimeter.

Figure 2. - Model instrumentation. (Dimensions in inches.)

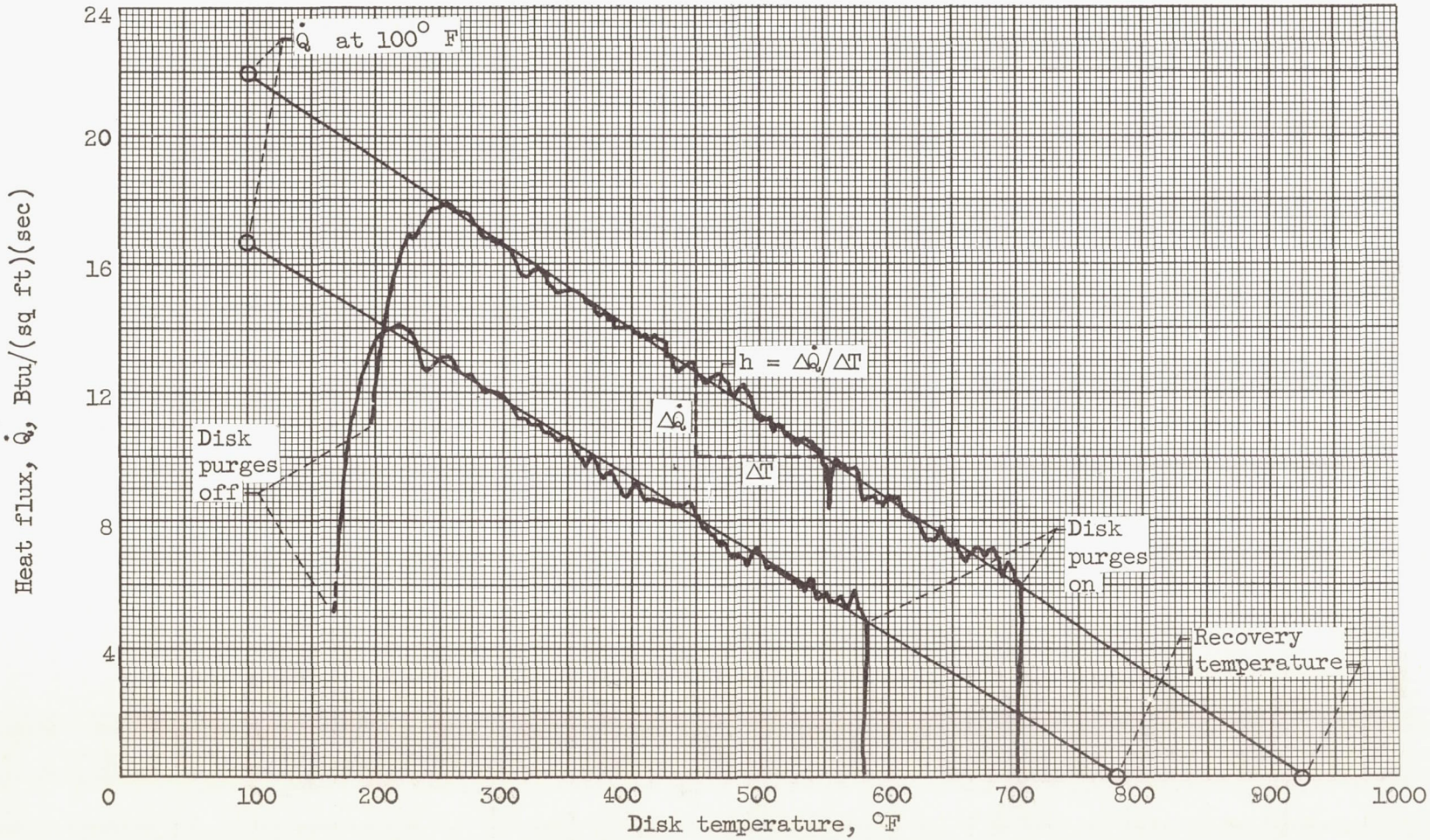

Figure 3. - Example traces of heat-flux variation with disk temperature made by electronic plotter. Absolute temperature, T; heat-transfer coefficient, h.

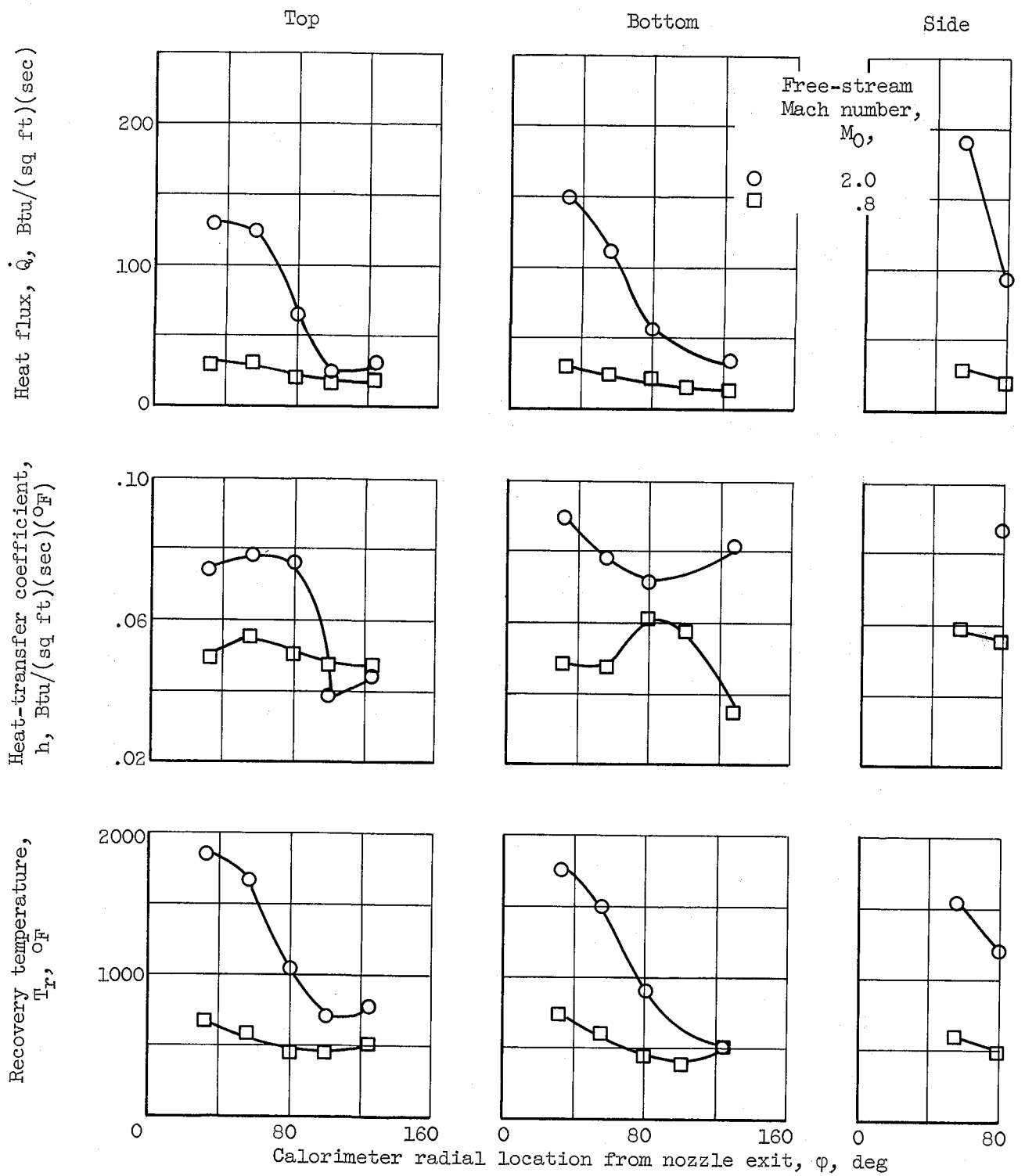

Figure 4. - Effect of free-stream Mach number on circumferential heat transfer. Chamber pressure, 200 pounds per square inch absolute; oxidant-fuel ratio, 2.35; angle of attack, 0^o.

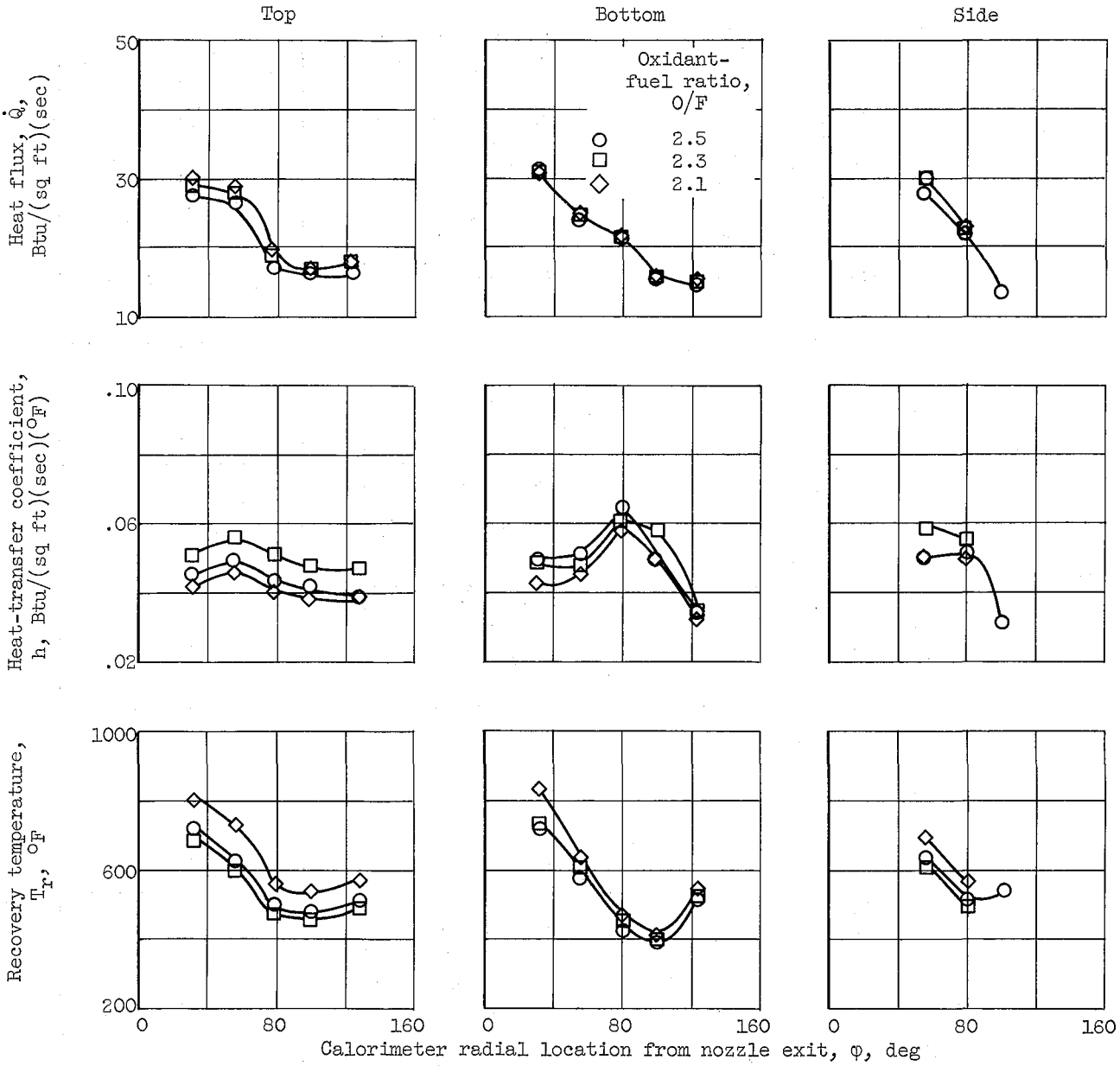

Figure 5. - Effect of oxidant-fuel ratio on circumferential heat transfer. Mach number, 0.8; chamber pressure, 200 pounds per square inch absolute; angle of attack, 0°.

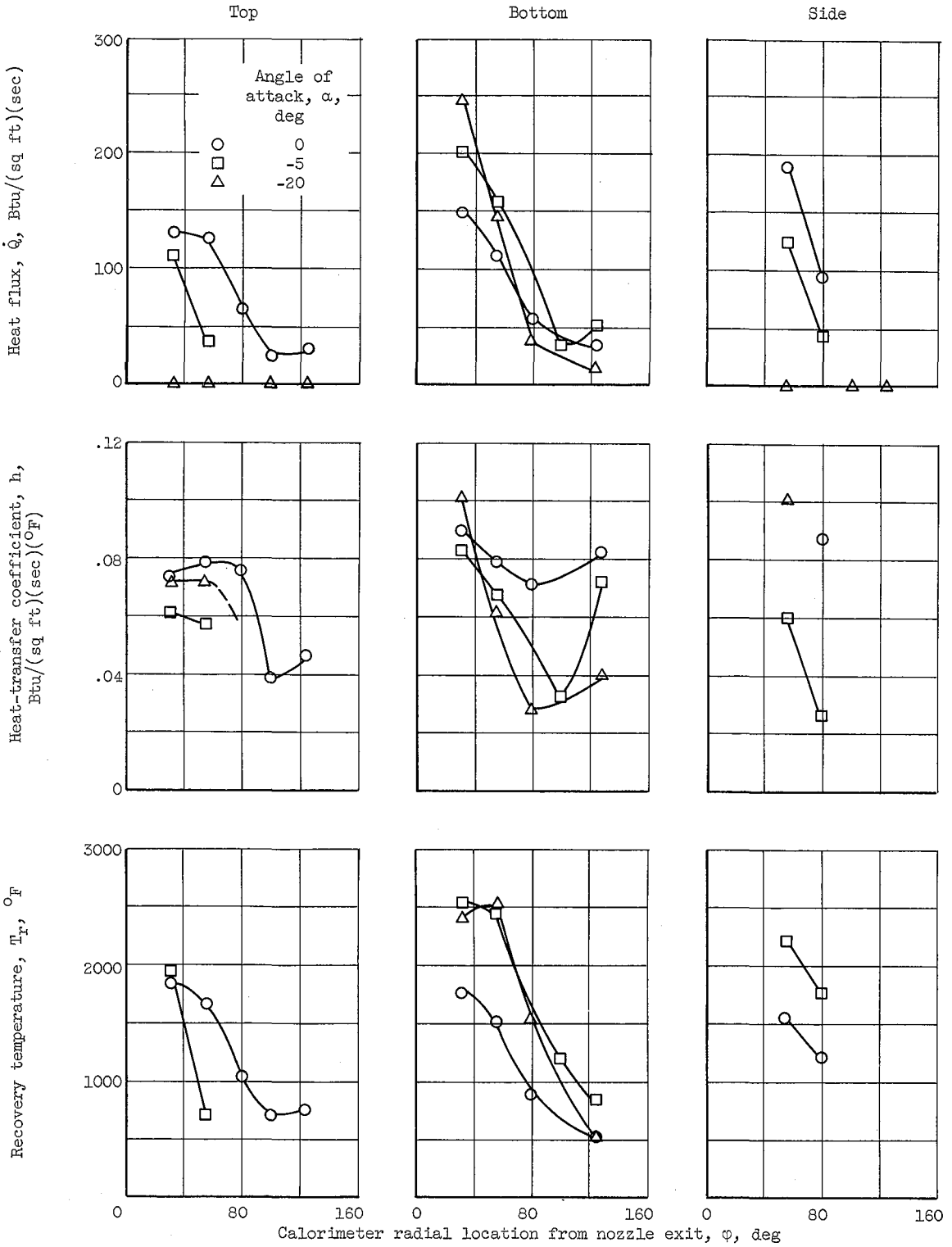

(a) Free-stream Mach number, 2.0.

Figure 6. - Effect of angle of attack on circumferential heat transfer. Chamber pressure, 200 pounds per square inch absolute; oxidant-fuel ratio, 2.35.

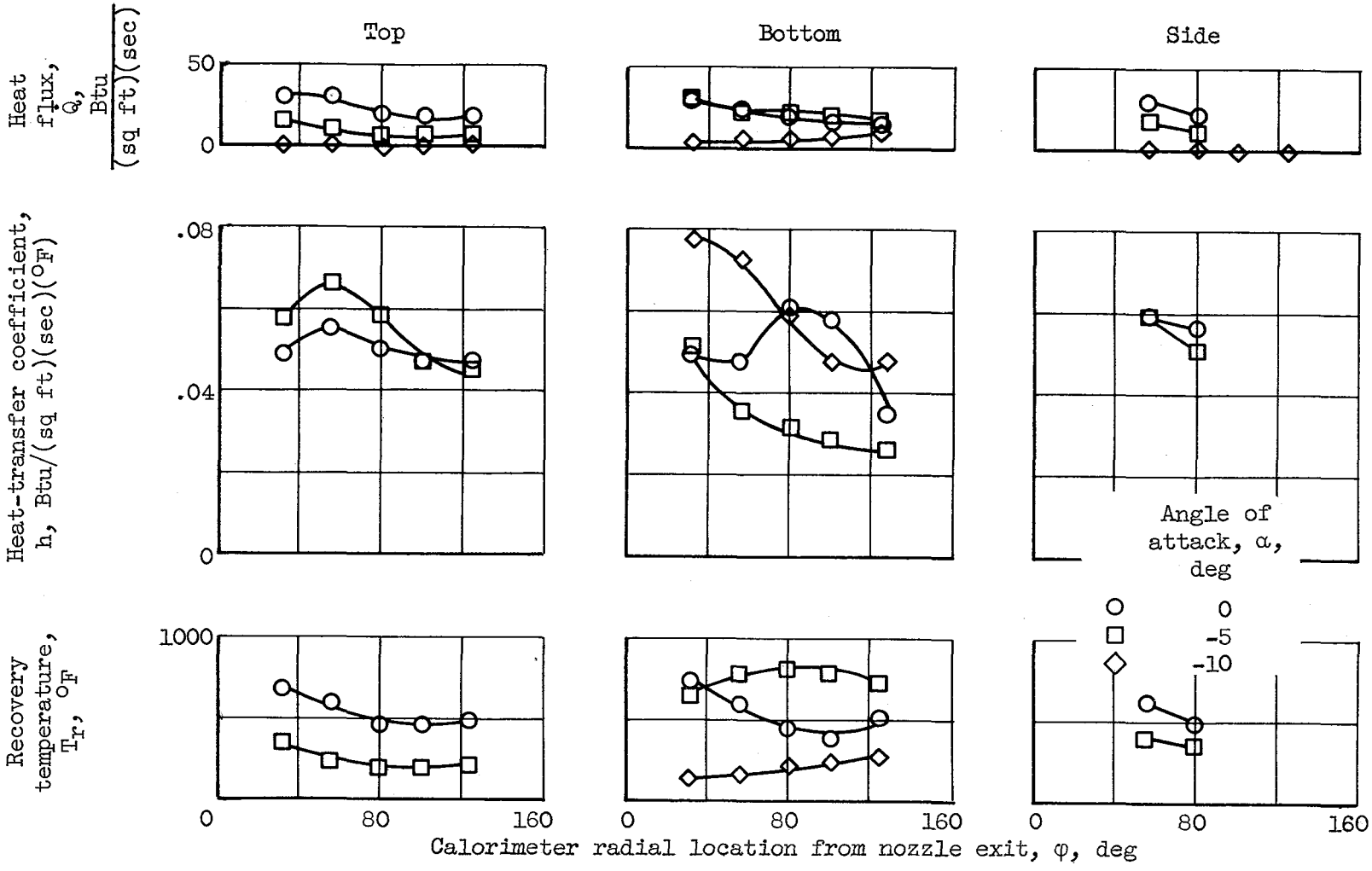

(b) Free-stream Mach number, 0.8.

Figure 6. - Concluded. Effect of angle of attack on circumferential heat transfer. Chamber pressure, 200 pounds per square inch absolute; oxidant-fuel ratio, 2.35.

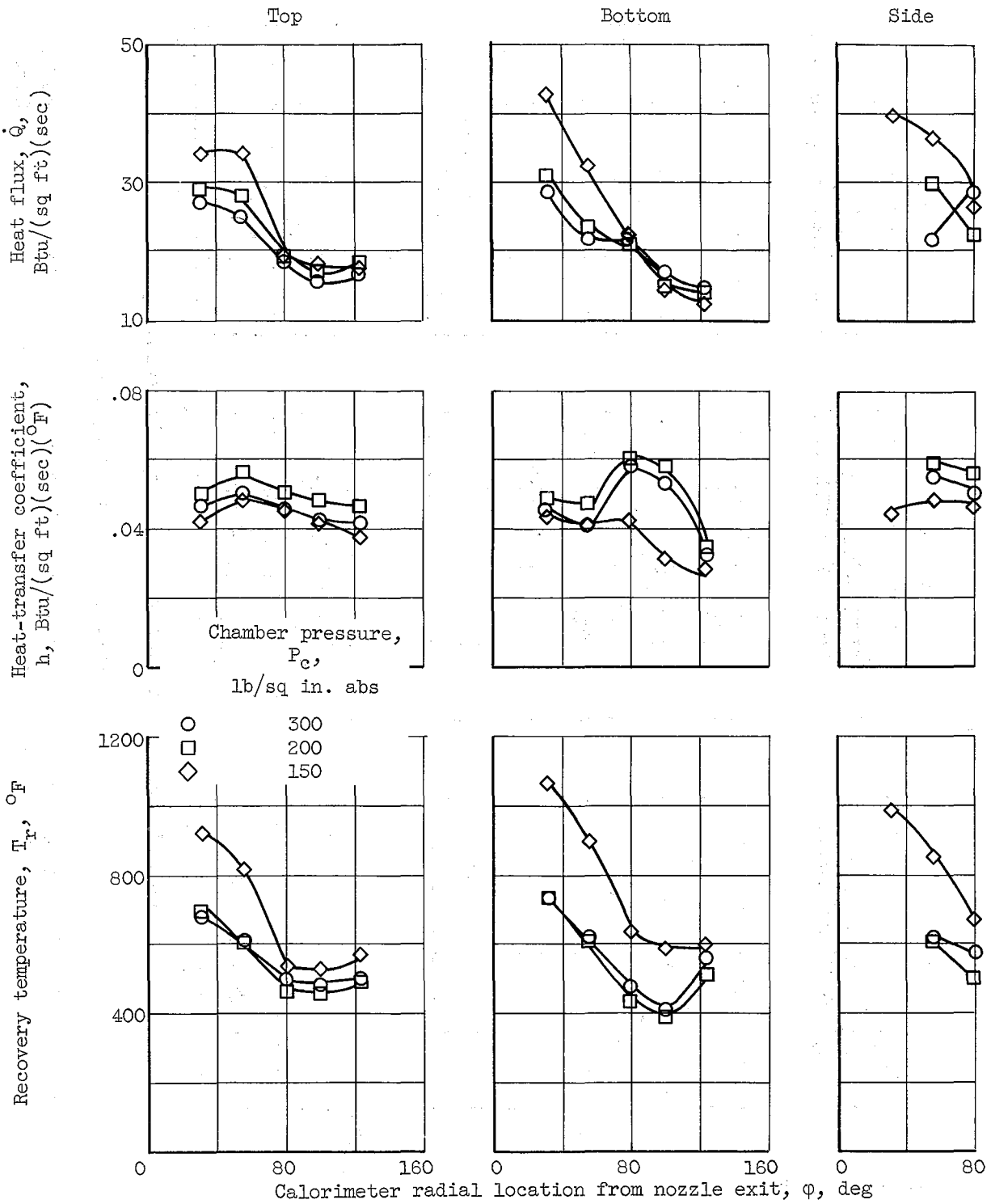

(a) Free-stream Mach number, 0.8; oxidant-fuel ratio, 2.3; angle of attack, 0^{o}.

Figure 7. - Effect of chamber pressure on circumferential heat transfer.

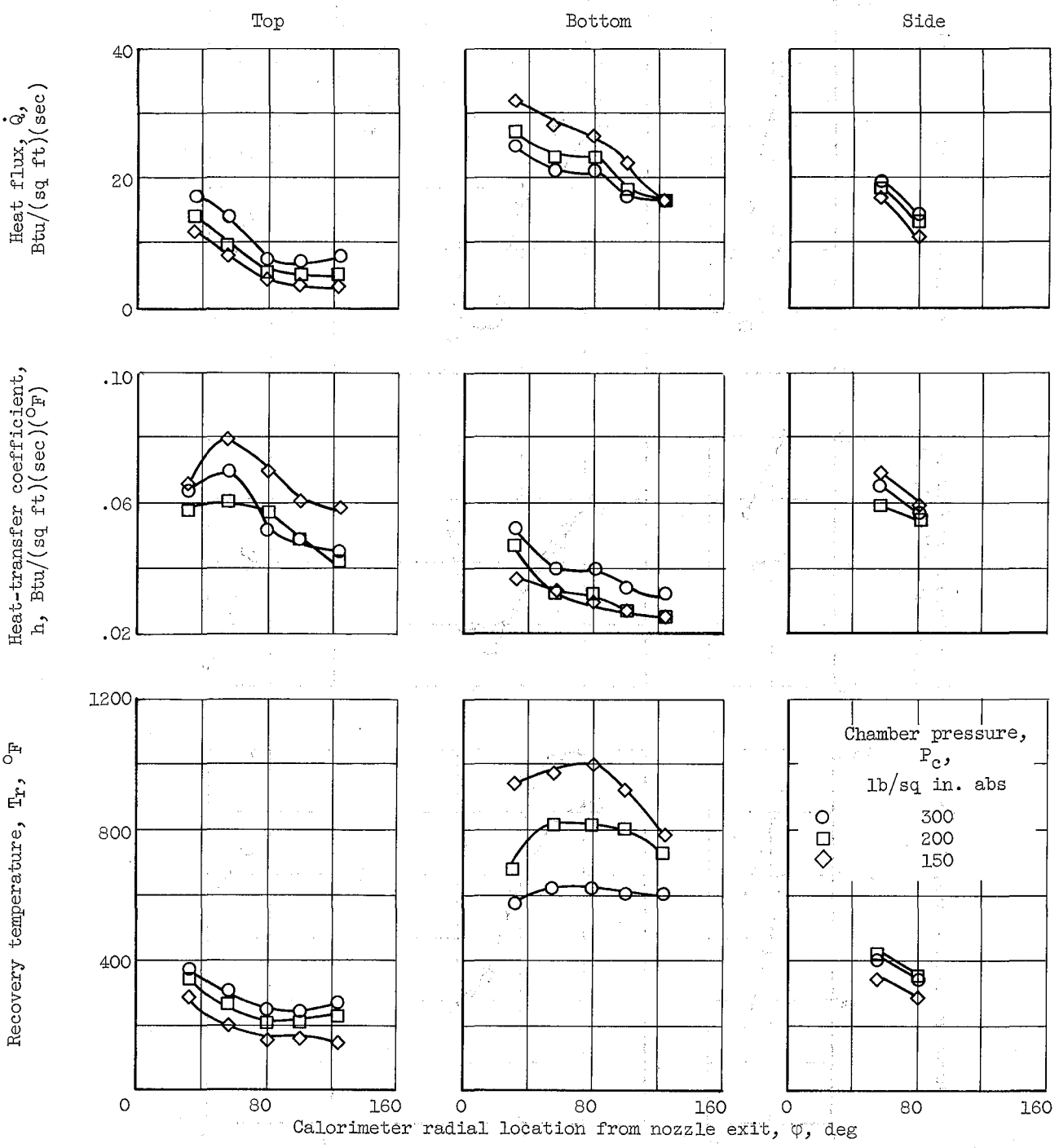

(b) Free-stream Mach number, 0.8; oxidant-fuel ratio, 2.35; angle of attack, -5°.

Figure 7. - Continued. Effect of chamber pressure on circumferential heat transfer.

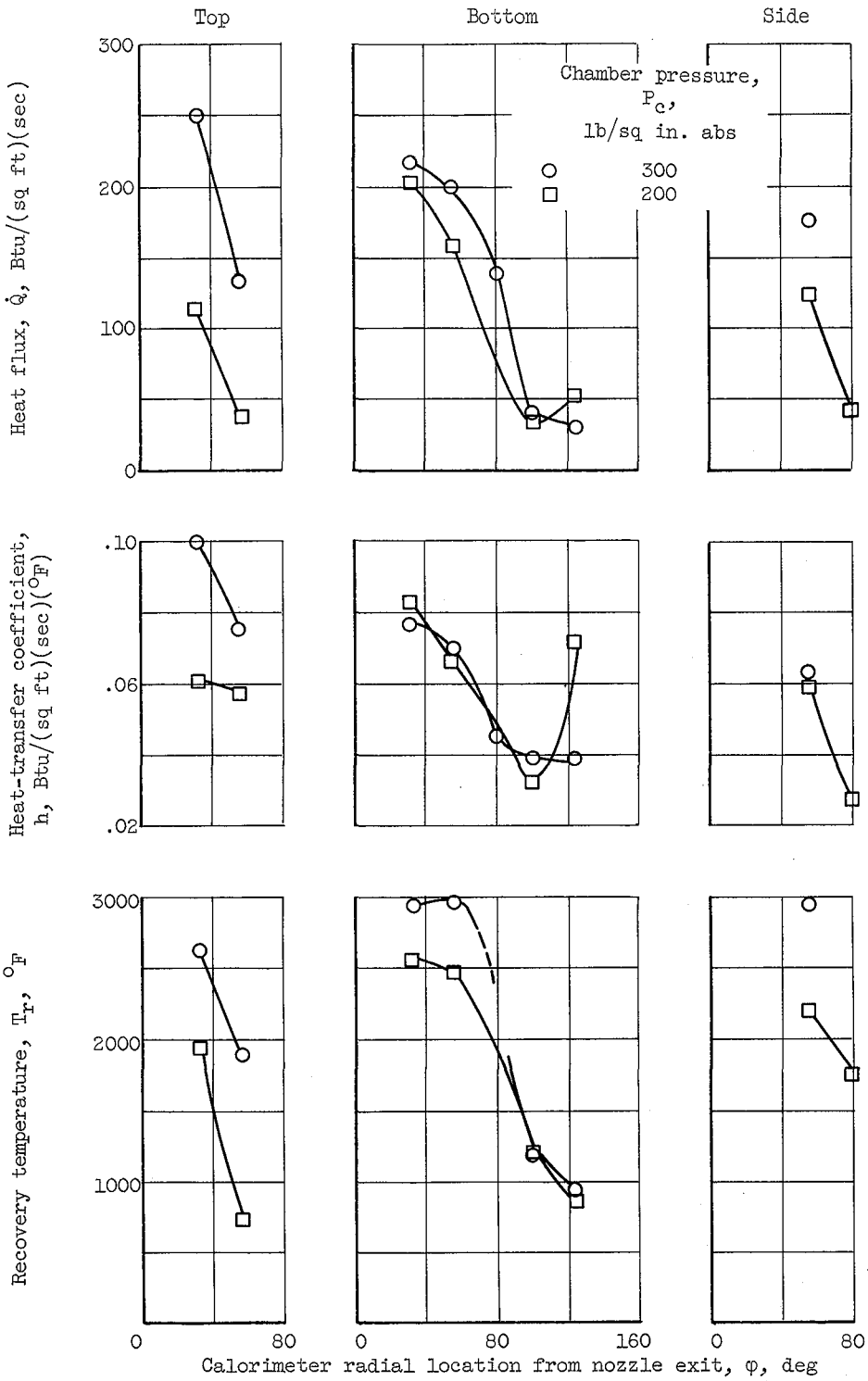

(c) Free-stream Mach number, 2.0; oxidant-fuel ratio, 2.35; angle of attack, -5°.

Figure 7. - Concluded. Effect of chamber pressure on circumferential heat transfer.

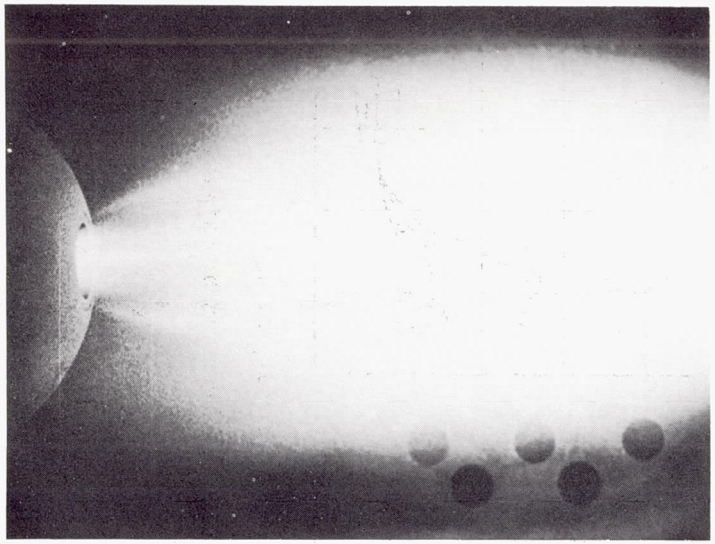

(a) Free-stream Mach number, 2.0; angle of attack, 0°.

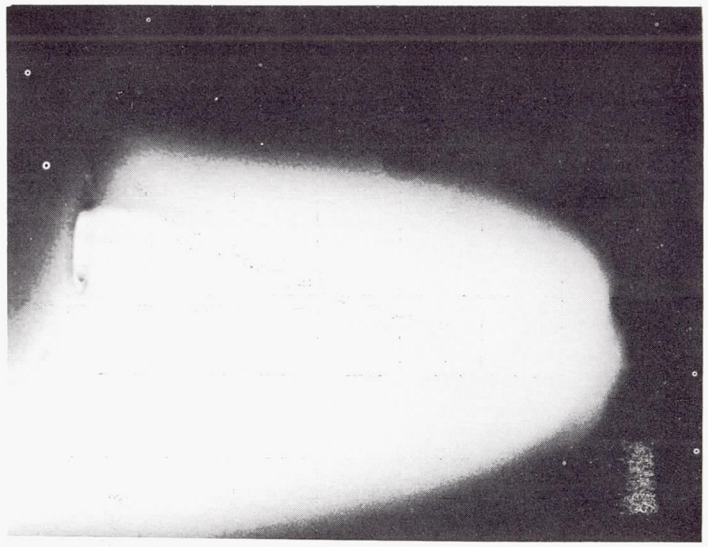

(b) Free-stream Mach number, 2.0; angle of attack, -5°.

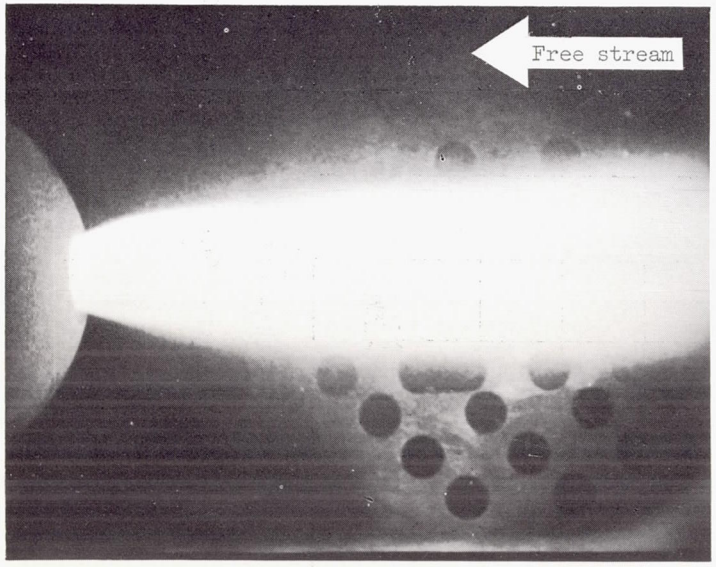

(c) Free-stream Mach number, 0.8; angle of attack, 0°.

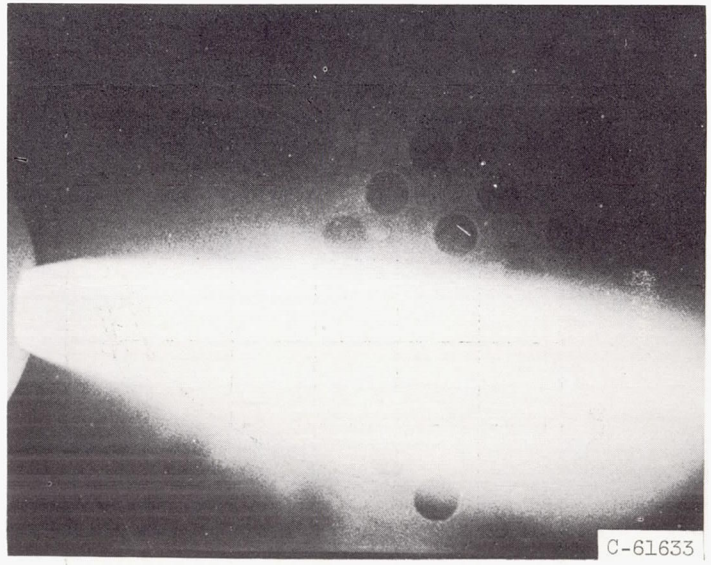

(d) Free-stream Mach number, 0.8; angle of attack, -5°.

Figure 8. - Jet shapes during test firings. Chamber pressure, 200 pounds per square inch; oxidant-fuel ratio, 2.4.

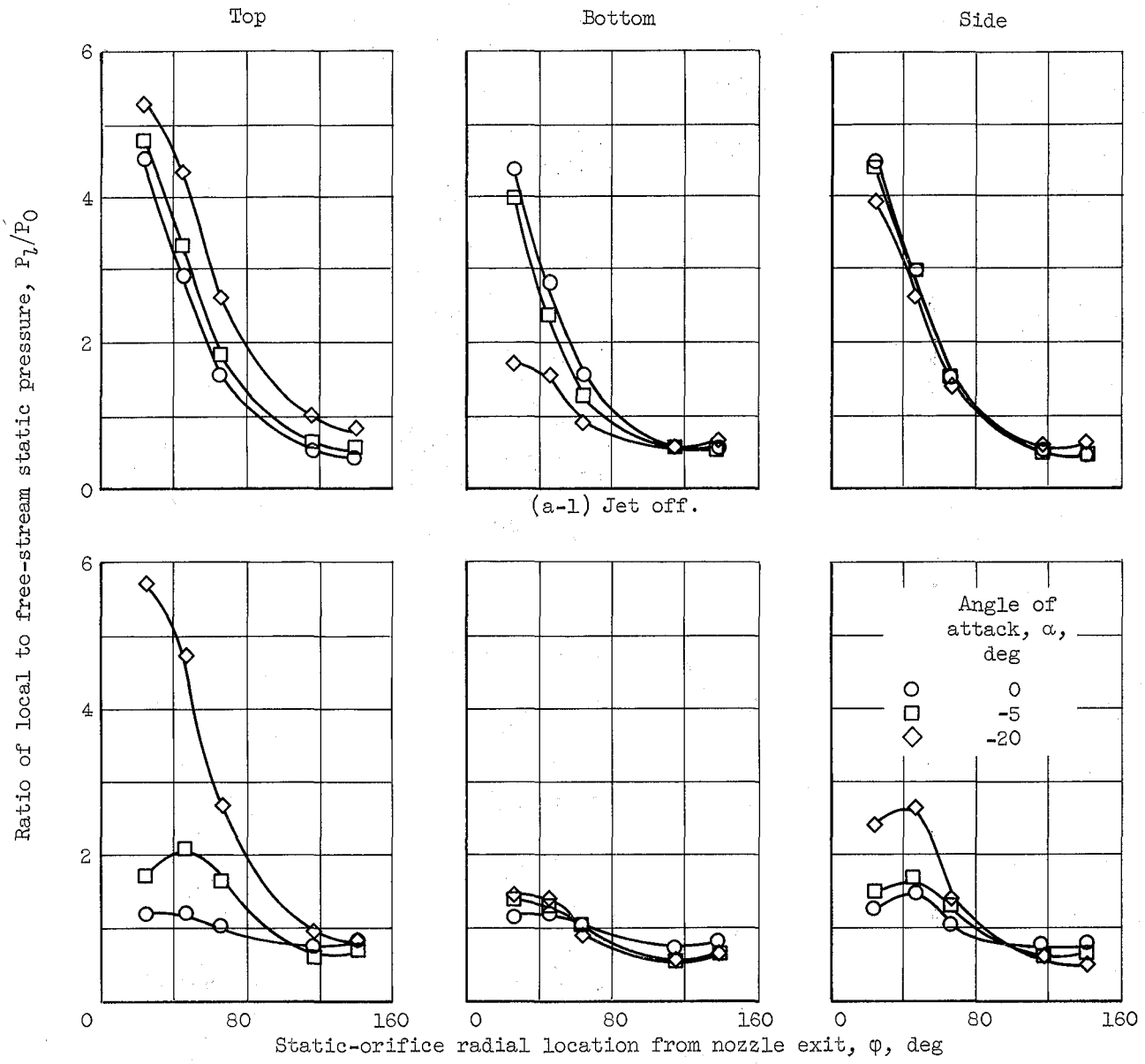

(a-2) Jet on. Chamber pressure, 200 pounds per square inch; oxidant-fuel ratio, 2.35.

(a) Free-stream Mach number, 2.0.

Figure 9. - Effect of angle of attack on circumferential pressure distribution.

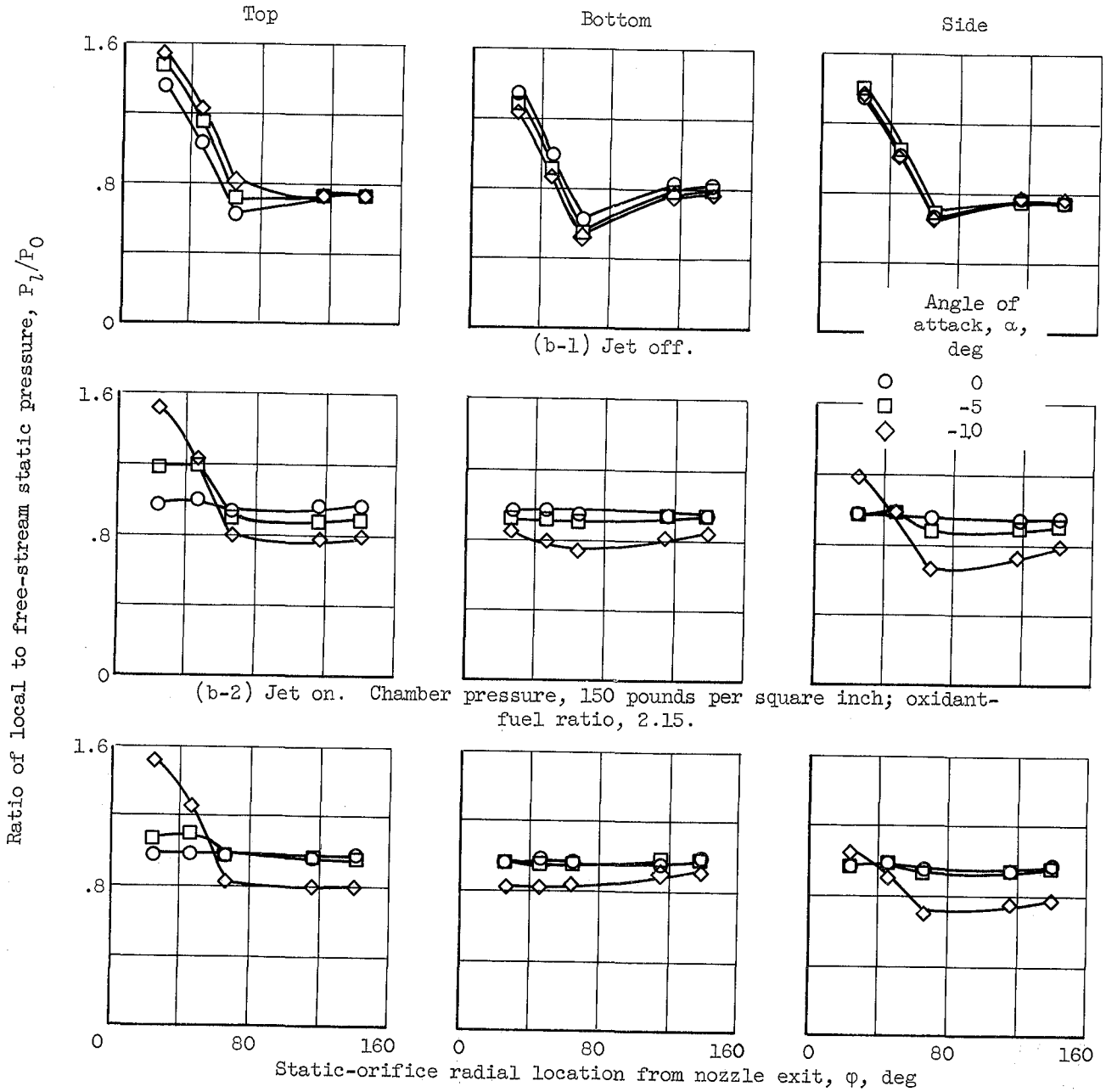

(b-1) Jet off.

(b-2) Jet on. Chamber pressure, 150 pounds per square inch; oxidant-fuel ratio, 2.15.

(b-3) Jet on. Chamber pressure, 300 pounds per square inch; oxidant-fuel ratio, 2.15.

(b) Free-stream Mach number, 0.8.

Figure 9. - Concluded. Effect of angle of attack on circumferential pressure distribution.